JOURNAL OF MATERIALS SCIENCE 26 (1991) 1247–1252

Silsesquioxane-derived ceramic fibres

F. I. HURWITZ, S. C. FARMER, F. M. TEREPKA
NASA Lewis Research Center, Cleveland, OH 44135, USA
T. A. LEONHARDT
Sverdrup Technology Inc., Cleveland, OH 44135, USA

Fibres formed from blends of silsesquioxane polymers were characterized to study the pyrolytic conversion of these precursors to ceramics. The morphology of fibres pyrolysed to 1400 °C revealed primarily amorphous glasses whose conversion to β-SiC is a function of both blend composition and pyrolysis conditions. Formation of β-SiC crystallites within the glassy phase is favoured by higher than stoichiometric C/Si ratios, while carbothermal reduction of Si–O bonds to form SiC with loss of SiO and CO occurs at higher methyl/phenylpropyl silsesquioxane (lower C/Si) ratios. As the carbothermal reduction is assumed to be diffusion controlled, the fibres can serve as model systems to gain understanding of the silsesquioxane pyrolysis behaviour, and therefore are useful in the development of polysilsequioxane-derived ceramic matrices and coatings as well.

1. Introduction

Development of tough, flaw-insensitive ceramic matrix composites for use in structural applications at elevated temperatures requires the availability of small diameter, oxidation resistant, continuous fibres. Spinning of fibres from a polymeric precursor, followed by pyrolytic conversion to a ceramic form provides an economical route using existing technology, and one which offers potential for attainment of high purity. Mah *et al.* [1] have reviewed those ceramic fibres which are currently available and under development. These include Nicalon [2–13] (derived from a polycarbosilane) Tyranno [14–16] (similar to Nicalon but incorporating titanium cross-links), a number of oxide fibres based upon alumina and alumina with zirconia additions (FP and PRD 166) [17] and Nextel [18] fibres (which are comprised of varying ratios of boria, alumina and silica), and several fibres under development by Dow Corning and Textron Corporations – the Si–C Dow Corning MPS and Textron fibres [1], and the Si–C–N–O-containing MPDZ and HPZ fibres from Dow Corning [19, 20]. The two developmental Si–C fibres have not been studied extensively at elevated temperature; the other fibres mentioned all lose strength at 1000–1200 °C as a result of crystallization and grain growth in the case of the oxide fibres and loss of CO and SiO in Nicalon and Tyranno (both contain some oxygen intentionally introduced in a cross-linking step). The thermal stability of the Si–C–N–O compositions is still being evaluated.

Therefore, there is a continuing need for the development of small-diameter fibres which can be produced in continuous lengths and which might be stable and retain strength and elastic modulus to higher temperatures. The objective of the present work was to identify polymers suitable for fibre spinning in terms of their rheological behaviour, as well as to study the relationship between initial polymer composition and molecular structure and the composition and morphology of the resulting ceramic, with the goal of "tailoring" the ceramic through alterations in polymer chemistry.

Polymeric precursors to ceramics also are of interest for forming composite matrices and coatings. Polymer pyrolysis to a ceramic char is accompanied by loss of gaseous species. Because of their high surface-to-volume ratio, pyrolysis of polymeric fibres provides a convenient model system for studying the polymer to ceramic conversion process, and would provide understanding necessary to the development of matrices and coatings as well as lead to new fibres.

The emphasis of this paper is on the chemical and morphological characterization of fibres drawn from a silsesquioxane melt and pyrolysed in an argon atmosphere to 1400 °C to yield an Si–C–O fibre. As polymer fibres were hand-drawn, and therefore not of uniform or optimum diameter, no attempt at mechanical property determination was made. The starting polymers were blends of commercially available methyl and phenylpropyl polysilsesquioxanes having the general formula $RSiO_{1.5}$. Polymers were characterized by differential scanning calorimetry (DSC) and thermogravimetric analysis (TGA). Fibre chemistry, morphology and microstructure were determined using scanning electron microscopy (SEM), electron microprobe, transmission electron microscopy (TEM) and energy loss spectroscopy (ELS).

2. Experimental details

2.1. Fibre preparation

Polymethylsilsesquioxane and a phenylpropylsilsesquioxane copolymer having a phenyl to propyl ratio

0022–2461/91 $03.00 + .12

TABLE I Composition of polymer blends

Batch	Composition				Si/C
	wt %		mol %		
	PP[a]	M[b]	PP[a]	M[b]	
2	50	50	36	64	2.47
3	60	40	46	54	2.88
4	70	30	57	43	3.33
5	40	60	28	72	2.14
6	30	70	19	81	1.77

[a] Polyphenylpropylsilsesquioxane.
[b] Polymethylsilsesquioxane.

of 7:3 were obtained from Huls America Inc. and used without further purification. Melting points of the polymers, as determined by DSC (Perkin Elmer DSC 4 at a heating rate of 5 °C min^{-1}) were 53 and 48 °C for the methyl and phenylpropyl polymers, respectively. The polymers were blended in various ratios of phenylpropyl to methyl, as summarized in Table I. The polymer blends were melted and the temperature of the melt maintained at 120–130 °C for several hours. Fibres were hand drawn at 90–100 °C, and were irradiated with ultraviolet light of 254 nm wavelength, 12–15 mW cm^{-2}, to cross-link the fibre exterior so that the fibres could be cured thermally without remelting [21]. Irradiated fibres were placed in a graphfoil-lined alumina boat; cure and pyrolysis were carried out sequentially in a flowing purified argon atmosphere (containing nominally 1 p.p.m. O_2) to 1400 °C. The final temperature was maintained for periods of 30 min to 2 h. Cure and pyrolysis conditions were based on previously published microdielectric studies [21] and on TGA data obtained for each of the polymers using a Perkin Elmer System 7 at a heating rate of 10 °C min^{-1} in argon.

2.2. Chemical and microstructural characterization

Both hand-fractured and polished fibres were studied by SEM using Cambridge 200 Stereoscan and Jeol 840 microscopes equipped with Kevex EDS systems. Uncoated and gold-coated fibres were examined at voltages of 10 and 15 kV to minimize charging. EDS spectra of carbon coated samples were collected at 8 kV.

Fibres to be metallographically prepared were mounted in an epoxy resin containing alumina hard filler. Specimens were ground to a 20 μm finish, then lapped on a copper/epoxy lapping disc with 6 μm diamond. Further lapping employed polymeric discs to 3 μm diamond, followed by vibratory polishing using a hard synthetic pad and 3 μm diamond slurry. Final polishing was accomplished with a 0.5 μm diamond slurry on a high nap synthetic cloth for 6 h.

Fibres drawn from a 50:50 wt % mixture of polyphenylpropylsilsesquioxane and polymethylsilsesquioxane were examined in a Philips 400T microscope operated at 120 kV and equipped with a Gatan energy loss spectrometer and cold stage. TEM specimens were prepared by potting fibres in an Al_2O_3-containing ceramic adhesive, followed by standard techniques of sectioning, polishing and ion-beam thinning.

Electron probe analysis was performed using an accelerating potential of 10 kV and 0.1 μA specimen current. A 10 nm thick layer of aluminium was applied to the specimens by vacuum deposition prior to analysis to provide a conductive path to ground.

3. Results and discussion

3.1. TGA

Weight loss curves for polymethylsilsesquioxane and polyphenylpropylsilsesquioxane heated at 10 °C min^{-1} to 1500 °C are shown in Fig. 1. Both polymers initially lose some weight at 50–100 °C, determined previously [21] from infrared studies to result from condensation of hydroxyl groups. The methyl polymer loses weight primarily at 175 and 715 °C, with a smaller weight change at nominally 540 °C, while the phenylpropyl copolymer has its largest transitions at 237 and 480 °C. The low-temperature set of transitions coincides with curing, as observed by microdielectrometry [21], the second set with polymer pyrolysis. The large temperature difference between the pyrolysis transitions for the two polymers suggests different decomposition mechanisms for each.

Char yields of nominally 80% for the methyl polymer, and 72% for the phenylpropyl copolymer, were observed after heating the materials in argon to 1500 °C and maintaining the final temperature for 30 min.

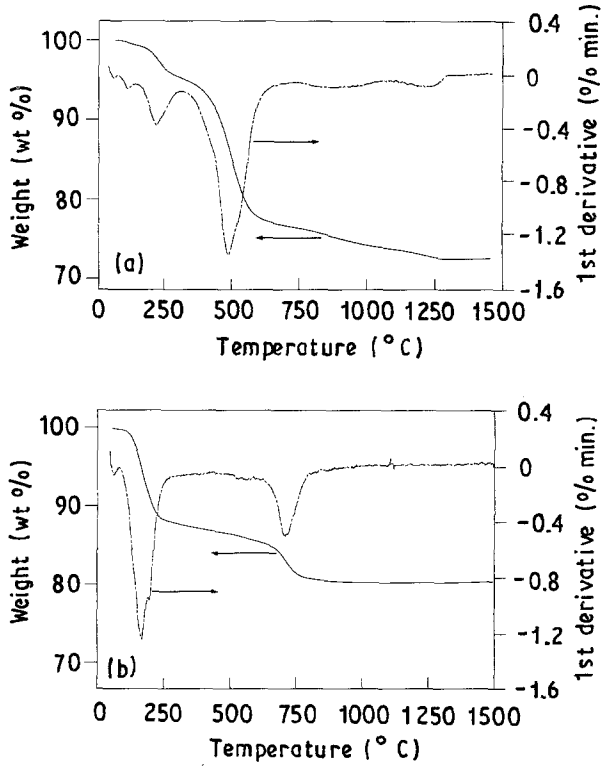

Figure 1 TGA curves showing weight loss of (a) polymethylsilsesquioxane and (b) polyphenylpropylsilsesquioxane at a heating rate of 10 °C min^{-1}.

3.2. Fibre preparation

Fibres were drawn from polymethylsilsesquioxane and polyphenylpropylsilsesquioxane alone and in blend ratios varying from 30/70 to 70/30 phenylpropyl/methyl, as described above. The methyl homopolymer does not cross-link when exposed to ultraviolet radiation at 254 nm. Therefore, it cannot be used alone, as it remelts on further heating. The phenylpropyl copolymer does react in the ultraviolet range; however it did not draw as uniformly as the methyl and phenylpropyl blends. The melt of the blends is characterized by droplets of one polymer within a clear melt of the other, which becomes white and opaque on stirring, indicative of their immiscibility.

3.3. Microstructural analysis

Blends containing 30–50 wt % phenylpropylsilsesquioxane formed oval to circular fibres, while those with higher phenylpropyl content produced fibres with more irregular shape (Fig. 2). The most circular fibres were observed for the 50/50 blend. The majority of the fibres exhibited longitudinal striations on their exterior surface (Fig. 2).

Fibre cross-sections as seen in back-scattered electron micrographs show a variety of two-phase morphologies (Fig. 3). Phase separation is observed for all blend ratios studied, the relative ratio of the two phases varying with the blend ratio. Microprobe analysis of polished sections indicates that the darker of these two phases seen in the SEM is the more carbon rich; this is attributed to the pyrolysis product of the phenylpropyl polymer, which would be expected to yield a higher concentration of carbon, while the lighter phase must derive primarily from polymethylsilsesquioxane.

On drawing fibres from the melt of the phenylpropyl/methyl blends, a flow pattern showing the two phases is seen along the fibre exterior of a polished longitudinal section (Fig. 4). As the phenylpropyl content of the blend is varied from 50/50 (Fig. 4a) to 30/70 phenylpropyl/methyl (Fig. 4b and c) phase inversion occurs, such that in the 50/50 blend the phenylpropylsilsesquioxane forms the continuous phase, whereas in the 30/70 material the phenylpropylsilsesquioxane copolymer is dispersed in a continuous polymethylsilsesquioxane phase.

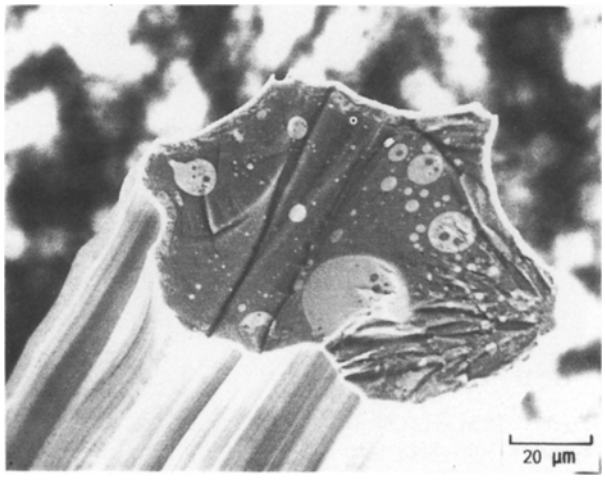

Figure 2 Fibre derived from blend of 60 phenylpropyl/40 methyl polysilsesquioxane pyrolysed to 1400 °C in flowing argon. Note irregular shape and longitudinal striations along the fibre.

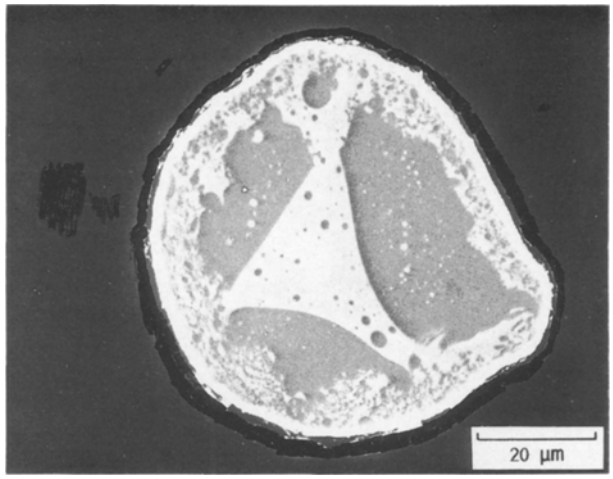

Figure 3 Typical polished cross-section of 50 phenylpropyl/50 methyl polysilsesquioxane blend fibre after pyrolysis to 1400 °C.

In TEM the morphology of the 50/50 blend (Batch 2) fibre consists of a uniform (ultraviolet cross-linked) exterior layer, ~ 300 nm thick, and a highly inhomogeneous interior as can be seen in Fig. 5. The fibre interior has phase separated. It is inferred from the flow line pattern of the longitudinal sections viewed in SEM that phase separation occurred during the early stages of fibre drawing. The dark phase has a higher Si/C ratio than the lighter regions as indicated by energy loss spectroscopy. (Note the contrast is opposite to that observed in SEM, where the darker phase is the more carbon rich). From TEM both light and dark phases are amorphous, the dark contrast arising from greater mass absorption of the silicon-rich phase.

The scale of separation between the two phases is spatially variable, being coarser and primarily spherical in the fibre centre, but more variably intermixed at the fibre exterior.

Although the fibre basically is amorphous, very small SiO_2 and β-SiC crystals were detected. The SiO_2 particles are 10–50 nm in size and appear as the small dark regions. Few such particles are observed. Of more interest, two regions of the fibre toward the fibre exterior showed a high density of randomly distributed β-SiC (Fig. 6). The SiC particles are ~ 20 nm in size and are observed solely in regions having a low Si/C ratio (light phase contrast in TEM).

TEM analysis of the interior regions of Batch 5 and 6 fibres, derived from 40/60 and 30/70 phenylpropyl/methyl blends, indicates that these fibres have a higher degree of crystallinity than was realized in Batch 2 (50/50) materials. β-SiC is detected throughout the fibre diameter. The microstructure seen in Fig. 7 is typical. The regions of lower Si/C content, seen in the lower left of the micrograph, contain a random distribution of SiC particles. The larger particles are 10 to 20 nm in size. The regions of higher Si/C content (upper right side of the micrograph) also contain a

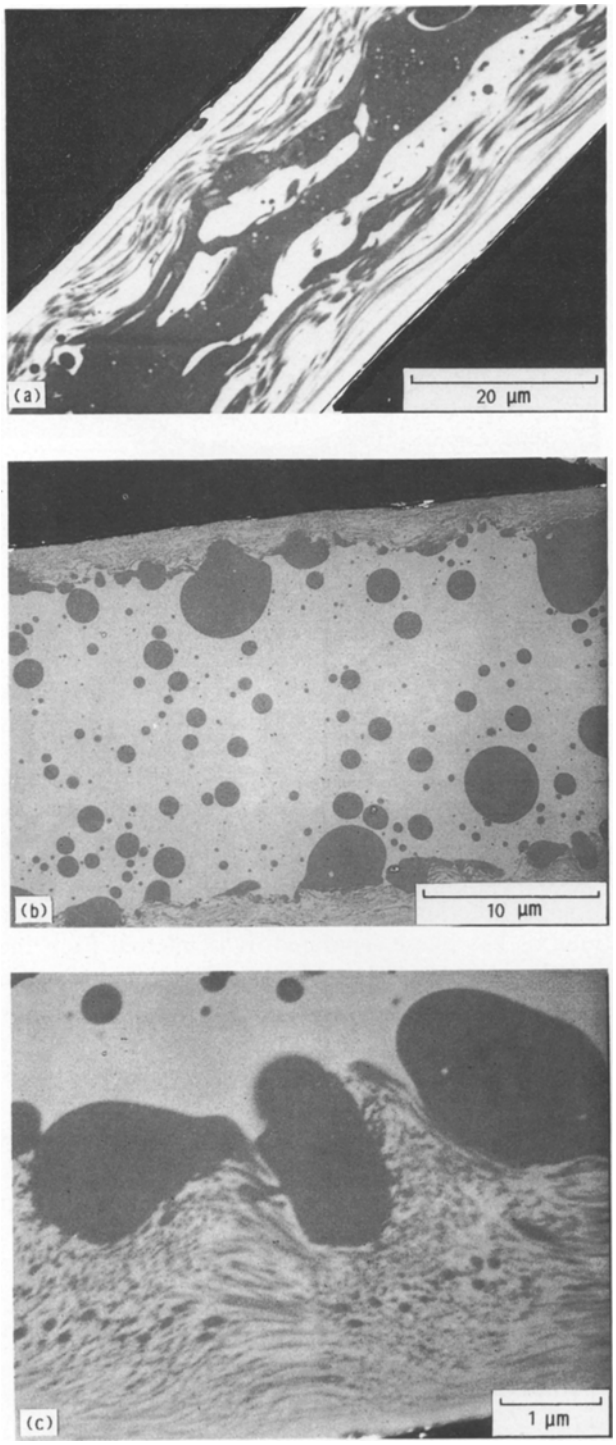

Figure 4 Polished longitudinal sections of (a) 50 phenylpropyl/50 methyl, and (b) and (c) 30 phenylpropyl/70 methyl polysilsesquioxane blend fibres following pyrolysis to 1400 °C. Change in blend ratio results in inversion of phases.

random distribution of β-SiC; however, the particle size is much smaller. The largest particles measured in this region were ~ 3 nm, as determined from dark-field micrographs. Phase separation of low Si/C and high Si/C regions occurred on a coarser scale than in Batch 2 fibres, as might be expected from the blend ratio.

Changes in blend ratio also produced differences in morphology at the fibre exterior. At a 40/60 ratio of phenylpropyl to methyl (Batch 5), a reaction zone forms around the circumference of the fibre after

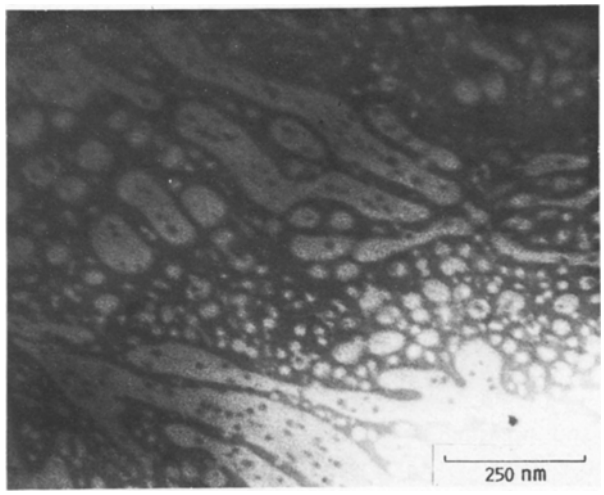

Figure 5 TEM foil of 50 phenylpropyl/50 methyl polysilsesquioxane fibre showing phase separation into regions of high Si/C (dark contrast) and low Si/C (light contrast).

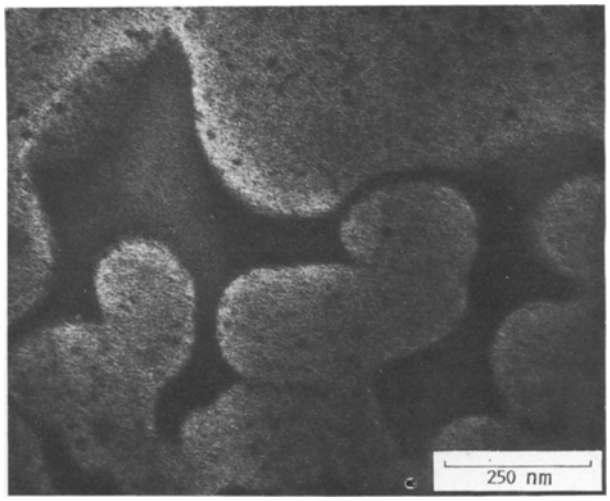

Figure 6 Region of 50 phenylpropyl/50 methyl polysilsesquioxane-derived fibre containing β-SiC crystallites in a low Si/C region near the fibre exterior.

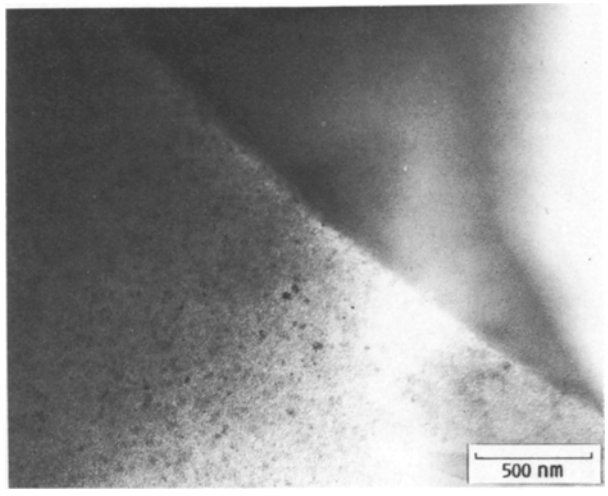

Figure 7 TEM foil of 30 phenylpropyl/70 methyl polysilsesquioxane-derived fibre. Both light and dark contrast regions contain a random distribution of small β-SiC particles. In the region at the lower left the particles are 10–20 nm in size and clearly visible. The particles at upper right are of much smaller size. Maximum particle size here is ~ 3 nm as measured in dark-field images.

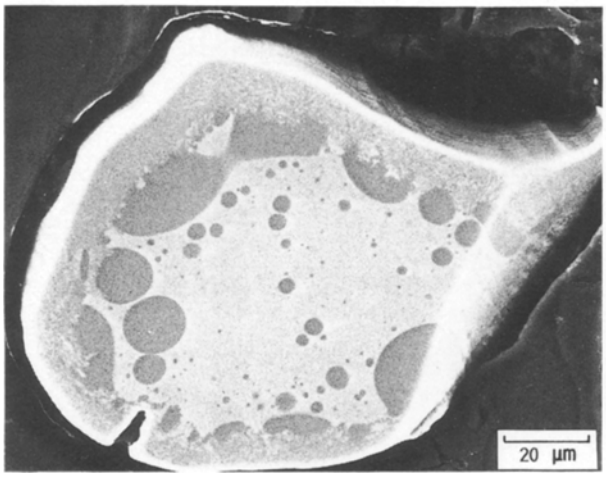

Figure 8 Polished cross-section of 40 phenylpropyl/60 methyl polysilsesquioxane fibre showing the reaction zone at the fibre exterior.

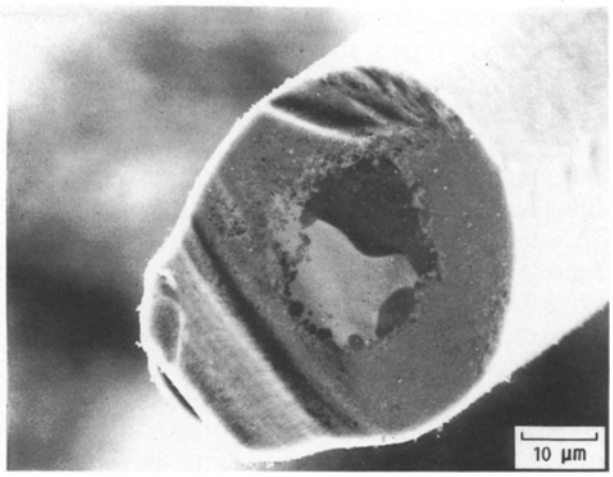

Figure 9 Fracture surface of 30 phenylpropyl/70 methyl polysilsesquioxane-derived fibre.

pyrolysis to 1400 °C for 2 h, as observed in SEM (Fig. 8). This reaction is not seen in the 50/50 blend. Microprobe analysis of the Batch 5 fibre (Table II) indicates the composition of the light and dark phases is identical to that seen in the Batch 2 blend. The composition of the reaction zone showed some local variation. In most small areas analysed by microprobe the oxygen content had diminished considerably compared with the fibre interior, though at least one location showed substantial oxygen content, as did larger regions of the reaction zone examined by energy dispersive spectroscopy. Some locations are carbon-rich compared to SiC, by probe analysis; in others, what appear to be carbon particles are noted.

Further decrease in phenylpropyl content to 30/70 by weight (Batch 6) produced a fibre in which the majority of the cross-sectional area had reacted after only 30 min at 1400 °C (Fig. 9). These fibres were weaker in handling than their Batch 2 or Batch 5 counterparts. Fracture surfaces of the Batch 6 fibres indicate that failure initiates from flaws within the reaction zone.

Formation of this reaction zone may be attributed to the conversion of $C_xSi_yO_z$, a material of unspecified composition at intermediate temperature (1000–1200 °C), to form SiC, with loss of SiO and CO [22–23]. The reaction is probably diffusion controlled. A final equilibrium composition of 39Si, 44C would be predicted for fibres maintained at this temperature for longer times, assuming loss of the remaining oxygen as CO, consistent with thermodynamic calculations [22].

A $C_xSi_yO_z$ oxycarbide phase has been proposed for Nicalon fibres [23] derived from oxidatively cross-linked polycarbosilanes. The existence of an oxycarbide phase in the fibres in the present study would be consistent with the position of the C peak intermediate between glassy carbon and C in SiC observed in the microprobe.

The reduction of SiO_2 by C is well known, and has been proposed to follow the reactions [22, 24]

$$SiO_2 + 3C \rightarrow SiC + 2CO \quad (1)$$

$$SiO_2 + C \rightarrow SiO + CO \quad (2)$$

and

$$SiO + 2C \rightarrow SiC + CO \quad (3)$$

A silicon oxycarbide phase also might be expected to produce SiC, SiO, CO and free C by a similar mechanism. Because the methyl polymer has a Si/C ratio of 1.0, while the phenylpropyl copolymer has a ratio of 5.1, the preferential formation of β-SiC in low Si/C regions is consistent with the above reaction scheme.

Despite the expected loss of SiO and CO, and the increase in Si/C content and decrease in O content found by microprobe analysis of this zone, porosity does not appear to be greater than that in the fibre interior. A similar lack of apparent porosity despite the loss of N_2, SiO and CO has been noted in the Si–C–N–O fibres prepared from organosilicon polymers [19].

TABLE II Composition of fibres, as determined by microprobe analysis, following pyrolysis to 1500 °C, with the final temperature maintained for 30 min

	At % (S.D.)		
	Si	C	O
Batch 2 (50PP/50M)[a]			
Light phase	28.2 (1.0)	28.1 (2.6)	43.7 (1.9)
Dark phase	18.5 (0.2)	52.2 (0.4)	29.3 (0.4)
Batch 5 (40PP/60M)[a]			
Light phase	28.8 (0.3)	26.5 (0.8)	44.8 (1.1)
Dark phase	18.8 (0.3)	51.8 (0.6)	29.4 (0.8)
Reaction zone			
A	0.1 (0.1)	95.0 (0.6)	4.9 (0.6)
B	39.3 (2.4)	52.2 (4.5)	8.0 (1.4)
C (single point)	36.7	36.1	26.7

[a] PP = polyphenylpropylsilsesquioxane, M = polymethylsilsesquioxane.

4. Summary and conclusions

A combination of the SEM and TEM results shows that what appear as homogeneous phases at a level of several micrometres (SEM) are actually an average of a phase-separated material at the nanometre (TEM)

level. The sharp contrast in the back-scattered image would seem to suggest that the two polymers are only partially miscible in the melt, with the lighter (SEM) phase being the more methyl-rich, and the darker having the greater phenylpropylsilsesquioxane concentration. Phase separation occurs into regions of both high and low Si/C ratio within drawn fibres. Separation occurs on a fine scale and the distribution of phases is highly variable.

The Batch 2 (50 phenylpropyl/50 methyl) fibres are essentially amorphous, but do contain some β-SiC in low Si/C regions toward the fibre exterior, possibly preceding or concurrent with the beginning of reaction at the fibre surface. In 40/60 and 30/70 blend fibres, β-SiC is detected throughout the fibre, and may be related to a diffusion-controlled carbothermal reduction. β-SiC crystal size was significantly larger in the low Si/C regions. The greater ease of formation of β-SiC in these areas may be related to differences in the level of phase separation and intermixing of the two polymers and the phase inversion observed with increases in methyl content of the blends.

In blend ratios containing at least 50 wt % polyphenylpropylsilsesquioxane the fibres persist as predominantly amorphous silicon oxycarbide glasses to at least 1400 °C, while at lower phenylpropyl concentrations reaction to form SiC and free carbon can occur, and the entire fibre converted if heat-treatment times and/or temperatures are increased. Thus polysilsesquioxanes can serve as precursors to both silicon oxycarbide and SiC fibres, depending on blend composition and pyrolysis conditions. By the same token, they can be useful high char yield (70–80%) precursors to ceramic matrix materials in fibre-reinforced ceramic composites or as fibre coatings.

Although the coarse phase separation observed here is not likely to be desirable in a high-temperature fibre, the level of homogeneity might be increased by high shear mixing techniques. Single-phase fibres with controlled phenyl/methyl ratios also can be produced from silsesquioxane copolymers. Future work will focus on control of copolymer composition and properties, and their relationship to fibre spinnability and ceramic stoichiometry and mechanical behaviour.

Acknowledgements

The authors thank Ju Young Chung and Dr Pirouz Pirouz, Case Western Reserve University, for preparation of TEM foils, Dr Arthur Heuer, Case Western Reserve University, David R. Hull, NASA Lewis Research Center, and Dr Linda Cornell for many helpful discussions of this work, John A. Setlock, Case Western Reserve University, for the energy dispersive spectroscopy analysis, and Lizbeth H. Hyatt for fibre preparation.

References

1. T. MAH, M. G. MENDIRATTA, A. P. KATZ and K. S. MAZDIYASNI, *Amer. Ceram. Soc. Bull.* **66** (1987) 304.
2. S. M. JOHNSON, R. D. BRITTAIN, R. H. LAMOREAUX and D. J. ROWCLIFFE, *J. Amer. Ceram. Soc.* **71** (1988) C132.
3. Y. HASEGAWA and K. OKAMURA, *J. Mater. Sci.* **18** (1983) 3633.
4. K. OKAMURA, M. SATO and Y. HASEGAWA, *J. Mater. Sci. Lett.* **2** (1983) 769.
5. H. ICHIKAWA, H. TERANISHI and T. ISHIKAWA, *ibid.* **6** (1987) 420.
6. G. SIMON and A. R. BUNSELL, *J. Mater. Sci.* **19** (1984) 3649.
7. G. SIMON and A. R. BUNSELL, *ibid.* **19** (1984) 3658.
8. T. J. CLARK, M. JAFFE, J. RABE and N. R. LANGLEY, *Ceram. Engng Sci. Proc.* **7** (1986) 914.
9. L. C. SAWYER, R. T. CHEN, F. HAIMBACH IV, P. J. HARGET, E. R. PRACK and M. JAFFE, *ibid.* **7** (1986) 914–930.
10. T. J. CLARK, E. R. PRACK, M. I. HAIDER and L. C. SAWYER, *ibid.* **8** (1987) 717.
11. Y. SASAKI, Y. NISHINA, M. SATO and K. OKAMURA, *J. Mater. Sci.* **22** (1987) 443.
12. T. MAH, N. L. HECHT, D. E. McCULLUM, J. R. HOENIGMAN, H. M. KIM, A. P. KATZ and H. A. LIPSITT, *ibid.* **19** (1984) 1191.
13. K. OKAMURA, T. MATSUZAWA and Y. HASEGAWA, *J. Mater. Sci. Lett.* **4** (1985) 55.
14. D. B. FISCHBACH, P. M. LEMOINE and G. V. YEN, *J. Mater. Sci.* **23** (1988) 987.
15. Y.-C. SONG, Y. HASEGAWA, S. J. YANG and M. SATO, *ibid.* **23** (1988) 1911.
16. T. YAMAMURA, T. ISHIKAWA, M. SHIBAUYA, T. HISAYUKI and K. OKAMURA, *ibid.* **23** (1988) 2589.
17. J. C. ROMINE, *Ceram. Engng Sci. Proc.* **8** (1987) 755.
18. D. D. JOHNSON, A. R. HOLTZ and M. P. GRETHER, *ibid.* **8** (1987) 744.
19. J. LIPOWITZ, H. A. FREEMAN, R. T. CHEN and E. R. PRACK, *Adv. Ceram. Mater.* **2** (1987) 121.
20. L. C. SAWYER, M. JAMIESON, D. BRIKOWSKI, M. I. HAIDER and R. T. CHEN, *J. Amer. Ceram. Soc.* **70** (1987) 798.
21. F. I. HURWITZ, L. H. HYATT, J. GORECKI and L. D'AMORE, *Ceram. Engng Sci. Proc.* **8** (1987) 732; Also NASA TM 89893 (1987).
22. K. E. SPEAR, P. M. BENSON and C. G. PANTANO, in "High Temperature Materials Chemistry IV", edited by Z. A. Munir, D. Cubicciotti and H. Tagewa (The Electrochemical Society, Pennington, NJ, 1988) pp. 345–54.
23. L. PORTE and A. SARTRE, *J. Mater. Sci.* **24** (1989) 271.
24. J. J. BIERNACKI and G. P. WOTZAK, *J. Amer. Ceram. Soc.* **72** (1989) 122.

Received 12 September 1989
and accepted 9 April 1990